

## A novel programming circuit for memristors

Shengtao Tu <sup>a</sup>, Jinyu Li <sup>a</sup>, Yanyun Ren <sup>b</sup>, Qin Jiang <sup>a</sup>, Shisheng Xiong <sup>a,\*</sup>

<sup>a</sup> State Key Laboratory of ASIC and System, Micro Nano System Center, School of Information Science and Technology, Fudan University, Shanghai 200433, China

<sup>b</sup> 2020 X-Lab, Shanghai Institute of Microsystem and Information Technology, Chinese Academy of Science, Shanghai 200050, China

### ARTICLE INFO

#### Keywords:

Memristor  
Memristor programmer circuit  
Multi-level memristance  
Memristor crossbar

### ABSTRACT

Memristor has attracted a lot of interest due to its high processing speed, low power consumption and high integration ability, which is critical for electronic systems and memory-centric computing. However, the memristor programming circuit and strategy are still inflexible and complex, since the signal generator/collector and stimulate pulse must be carefully matched and designed based on memristor intrinsic characteristics without reconfigurable. Here, a simple and effective circuit only consists a parallel reference-resistor-and-NMOS is designed to program memristor with a >99% memristance precision. And the amplitude and width of stimulate pulse are fixed to  $\pm 4$  V and 5 ms, respectively. In order to cope with the device variation, such as  $\pm 10\%$  tolerance of transition voltage, an optimized programming strategy was proposed and demonstrated great robustness. Additionally, a set of reference resistors and NMOSs have been added to facilitate multi-level memristance operation without requiring any changes to the circuit structure. This program circuit was also employed to program memristor crossbar remains 99% precision. In the end, a memristor-based convolutional neural network which controlled by our optimized programming circuit was used for image recognition, and 89.36% accuracy can be achieved even under 15.8% memristance tolerance. This novel circuit demonstrates a simple and flexible strategy in memristor programming, providing a new way to control memristor crossbar for practical application.

### 1. Introduction

In 1971, the memristor is the fourth basic circuit element that is proposed by L. O. Chua in theory [1]. As the fourth basic circuit element besides resistor, capacitor, and inductor, memristor has been considered as one of the next generations of non-volatile memory technology. The memristor is a nonvolatile device and has variable memristance. When the current flows through the memristor from different directions, the memristance will change accordingly. When the current cross the memristor was removed, the memristance will remained. In 2008, the first physical memristor was reported by HP labs [2]. The phenomenon of resistive switching in electronic devices has attracted wide interest from academia and industry, due to its application to store information in a memristor, enabling the development of neuromorphic and memory-centric computing systems [3–11].

In recent years, programmable and reconfigurable analog elements have attracted considerable attention. There have been various studies on the memristor programmable circuit. In 2010, Pershin et al. developed a programmable memristor circuit that consists of a

microprocessor, analog-to-digital converter, and digital potentiometer [12]. In 2012, Berdan et al. presented an analog programming circuit for accurately setting the state of a memristor which exploited the dynamic modulation of resistance under a constant DC bias [13]. In 2016, Merced et al. investigated 1T1R memristor arrays rapidly reaching arbitrary conductance states and proposed an adaptive pulsed algorithm. The programming was performed by applying the algorithm which utilized the transistor gate voltage to control the SET switching operation [14]. Kim et al. suggested a tuning approach which exploited the voltage divider effect. The hardware structure is a resistor in series with the memristor [15–17]. In 2017, Olumodeji et al. presented a circuit for accurately programming the memristor which took advantage of the memristor's pulse-based programmability. The circuit program the memristor in both an incremental and a decremental fashion by using auto-tuning operational amplifier's gain [18]. Mokhtar et al. proposed a resistance writing circuit by applying a pulse-coded memristor programming method. It used 2 sets of switches to increase or decrease memristance by supplying a negative or positive pulse [19]. In 2020, Tarkhan et al. presented a novel CMOS circuit for programming

\* Corresponding author.

E-mail address: [sxiong@fudan.edu.cn](mailto:sxiong@fudan.edu.cn) (S. Xiong).



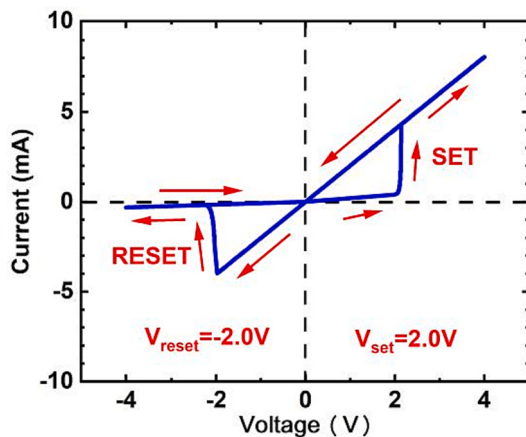


**Fig. 1.** Simulation I-V curve of the memristor.  $V_{set}$  is the positive threshold with the value of 2.0 V. When the voltage applied to the memristor is  $> 2.0$  V, the memristance decreases to  $R_{on}$  sharply.  $V_{reset}$  is the negative threshold with the value of  $-2.0$  V. When the voltage applied to the memristor is less than  $-2.0$  V, the memristance increases to  $R_{off}$  sharply.

memristors which exploited a Wheatstone bridge circuit to measure the current memristance [20]. In 2020, Daoud et al. suggested a high precision read and write circuit for memristors. The circuit has a feedback link which is used to read the final memristance. And it determines the required decision of switching the memristance to a lower or a higher memristance value [21]. In 2022, Knownm Inc. explored different circuit topologies and approaches to perform the forming of RRAM. A target-resistance was pursued through pulsed voltage source, followed by cycle-to-cycle stabilization using a custom trans-impedance amplifier circuit [22]. In 2023, Randrianantenaina et al. reported programmable and reconfigurable analog and digital platforms as an alternative perspective in order to promote analog and digital applications based on memristors [23].

In this paper, we suggest an approach to program memristors in analog circuits based on the threshold-type behavior of the memristor. Our main idea is to use a negative source to programs the memristor to high resistance states (HRS). The positive source then programs the memristor to aim memristance. In addition, we have added a reference resistor to program the memristor to multi-level memristance according to digital input signals. Finally, a convolutional neural network (CNN) has been trained by our circuit and 77.64% classification precision can be achieved even under 22.2% memristance tolerance. In this way, we obtain a programmable circuit that can obtain accurate memristance and has a simple structure.

## 2. The memristor programmable circuit

### 2.1. Memristor model

The adopted memristor model has been proposed by Pershin [24]. The memristor has a threshold characteristic. In other words, when the voltage applied to the memristor is greater than the threshold value, the memristance (memristor resistance) will change. Otherwise, the memristance will remains unchanged. The mathematical expressions of this model are as follows:

$$I(t) = R_M^{-1}(X, V_M, t)^* V_M(t) \quad (1)$$

$$\dot{X} = f(X, V_M, t) \quad (2)$$

$$I = X^{-1} * V_M \quad (3)$$

$$\frac{dX}{dt} = f(V_M) [\theta(V_M) \theta(R_{off} - X) + \theta(-V_M) \theta(X - R_{on})] \quad (4)$$

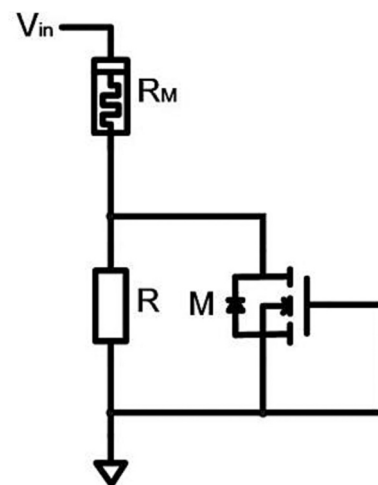


**Fig. 2.** Memristor programming circuit.  $R_M$  is the memristor that to be programmed,  $R$  is the reference resistor and  $M$  is the NMOS.

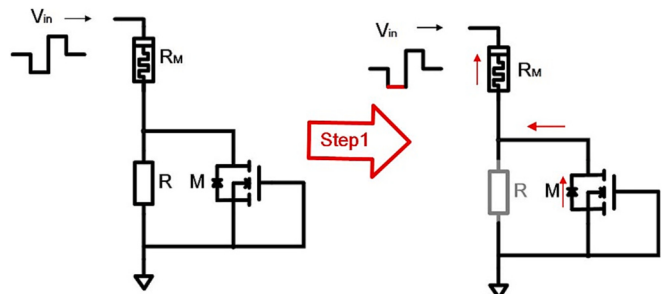


**Fig. 3.** Step 1 of the memristor programming process. In this period, input source  $V_{in}$  is negative. The current flows through  $M$  and  $R_M$ , as the red arrows in the picture. And the voltage applied to the memristor is negative. (For interpretation of the references to colour in this figure legend, the reader is referred to the web version of this article.)

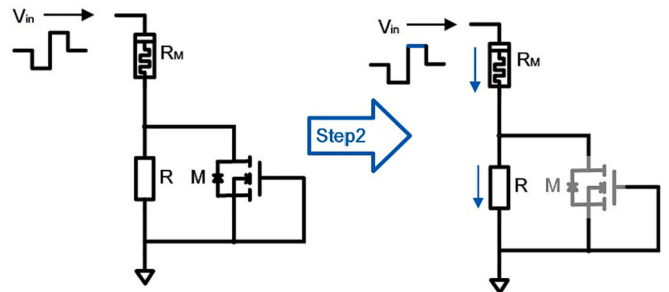


**Fig. 4.** Step 2 of the memristor programming process. In this period, input source  $V_{in}$  is positive. The current flows through  $R_M$  and  $R$ , as the blue arrows in the picture. And the voltage applied to the memristor is positive. (For interpretation of the references to colour in this figure legend, the reader is referred to the web version of this article.)

$$f(V_M) = \beta V_M + 0.5(\alpha - \beta)[|V_M + V_t| - |V_M - V_t|] \quad (5)$$

where  $X$  represents n-th internal state variables, and  $X$  is a vector.  $V_M(t)$  is the voltage applied to the memristor,  $I(t)$  is the current that flows through the memristor.  $V_t$  is the memristor threshold voltage.  $R_M$  is the memristance which is a scalar.  $R_{on}$  is the LRS and  $R_{off}$  is the HRS. The  $\theta(\bullet)$  are step functions that are used to limit the memristance to the region between  $R_{on}$  and  $R_{off}$ . The coefficients  $\alpha$  and  $\beta$  define the slopes of

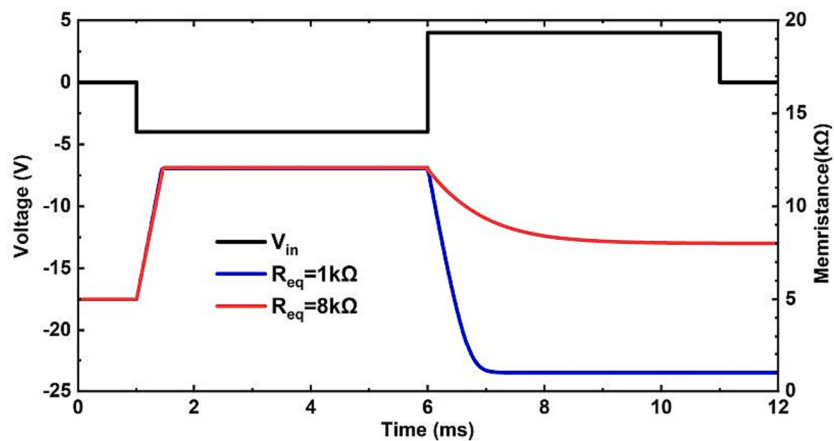


**Fig. 5.** Simulation of the programmable circuit. The black line is the input source  $V_{in}$ , and the value is  $-4.0\text{ V}$  during first 5 ms and  $4.0\text{ V}$  during second 5 ms of the pulse. The blue line represents the memristance when the reference resistor is  $R = 1\text{k}\Omega$ . The red line represents the memristance when the reference resistor is  $R = 8\text{k}\Omega$ . (For interpretation of the references to colour in this figure legend, the reader is referred to the web version of this article.)

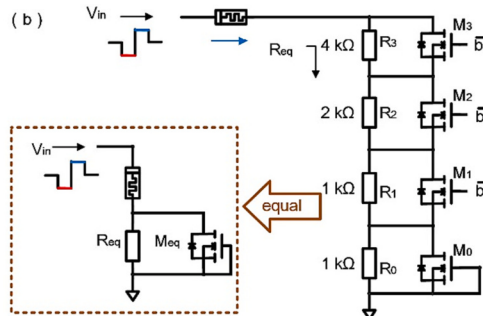
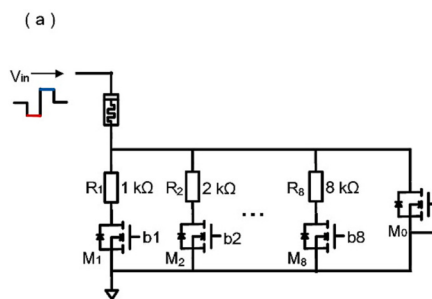


**Fig. 6.** Reference resistor circuit. (a) Reference resistors without series of parallel reference-resistor-and-NMOS structure. The reference resistor circuit with 8-input bits.  $R_1-R_8$  are reference resistors ;  $b1-b8$  are digital control signals. (b) Reference resistors with series of parallel reference-resistor-and-NMOS structure. The reference resistor circuit with 3-input bits.  $R_0$  ,  $R_1$  ,  $R_2$  ,  $R_3$  are reference resistors ;  $\overline{b3} \ \overline{b2} \ \overline{b1}$  are digital control signals. The circuit is equivalent to the circuit diagram in the dashed box.  $R_{eq}$  is an equivalent resistance.  $M_{eq}$  is an equivalent NMOS.

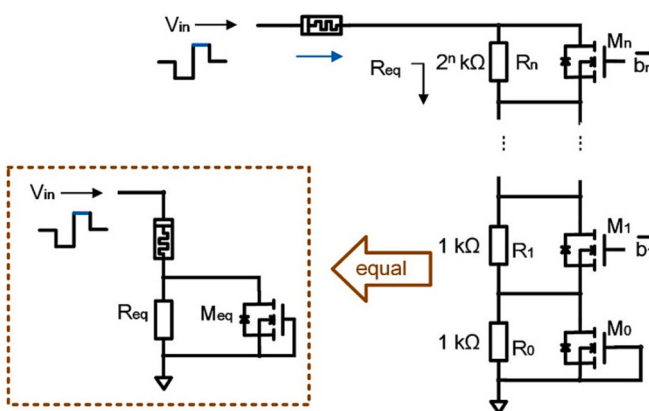


**Fig. 7.** The reference resistor circuit with  $n$ -input bits.  $R_0$  ,  $R_1$  , ... ,  $R_n$  are reference resistors ;  $\overline{b_n} \dots \overline{b_1}$  are digital control signals. The circuit is equivalent to a circuit diagram in the dashed box.  $R_{eq}$  is the equivalent resistance and  $M_{eq}$  is the equivalent NMOS.

the  $f(V_M)$  curve below and above the threshold, which characterize the rate of memristance change at  $|V_M|/V_t$  and  $|V_M|/V_t$ , respectively.

A positive or negative voltage applied to the memristor decreases or increases the memristance  $R_M$ . The device state changes only when  $|V_M|/V_t$  (for set transition  $V_t = V_{set}$ , and for reset transition  $V_t = V_{reset}$ ). As shown in Fig. 1, when the voltage value applied to the memristor is greater than the positive threshold of the memristor ( $V_M > V_{set}$ ), the memristance decreases sharply, memristor tends to change from HRS to LRS, and the process is SET transition, when the voltage value applied to

the memristor is less than the negative threshold of the memristor ( $V_M < V_{reset}$ ), the memristance increases sharply, memristor tends to change from LRS to HRS, and the process is RESET transition. (See .)

## 2.2. The memristor programmable circuit

In the programmable analog circuits of memristors, Pershin et al. developed a circuit that applied negative voltage to the memristors and then use positive voltage to program the memristor's states during their operation as analog circuit elements [12]. In addition, the voltage divider effect is usually used in programmable circuit [15–17]. This paper proposes a novel circuit by utilizing before design ideas and adding a reference resistor that is designed to be controllable. The circuit is simple and the memristance is configurable.

When programming the memristor, if the memristance is greater than the aim value, it is necessary to decrease the memristance through a SET process. If the memristance is less than the aim value, it is necessary to increase the memristance through a RESET process. Before programming the memristor, it is first to obtain the greatest memristance value  $R_{off}$  by RESET process. Then it programs the memristor to aim value. In addition, we also add a reference resistor which contributes to obtaining aim memristance, through this structure the memristance is configurable. The memristance is related to the reference resistor, and the reference resistor is controlled by digital input signals. The proposed memristor programmable circuit structure contains one memristor, one NMOS, and one reference resistor as shown in Fig. 2.  $R_M$  is the memristor,  $R$  is the reference resistor, and  $M$  is the NMOS, respectively.

The programming progress contains two steps:

Step 1: the input source  $V_{in}(|V_{in}| > |V_{reset}|)$  is negative. The current flows through NMOS (NMOS can be regarded as a diode) and then through memristor  $R_M$  to reset the memristor, as shown in Fig. 3. So, the

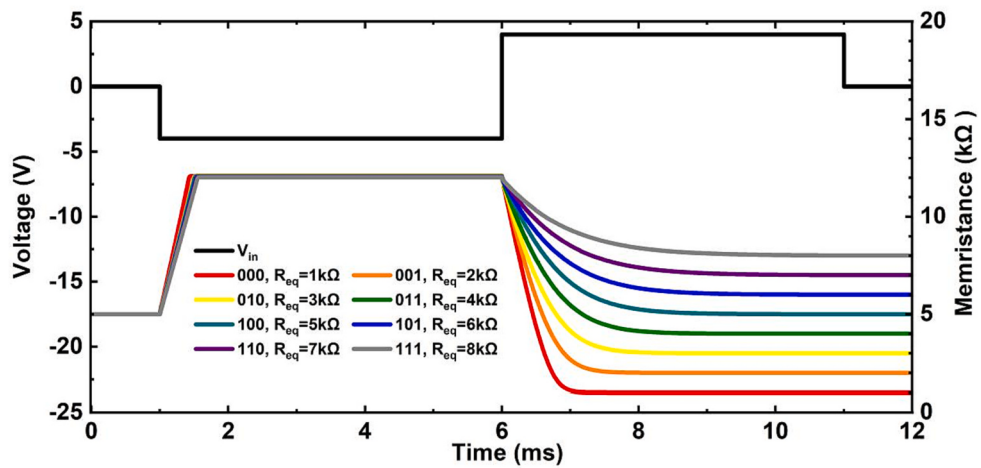


**Fig. 8.** Simulation of the programmable circuit according to different input signals. The black line is the input source  $V_{in}$ . And the colour lines are the memristances evolution as the function of different reference resistors.

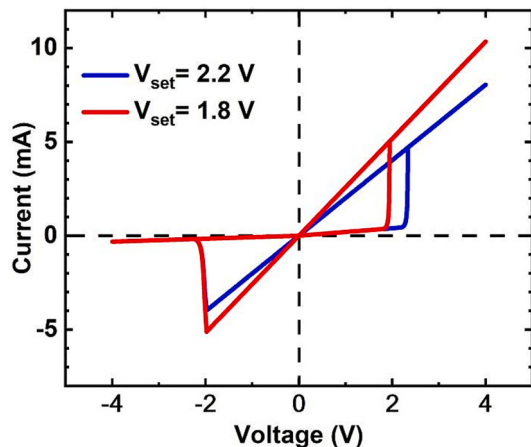


**Fig. 9.** Simulation I-V curve of the memristor. The red I-V curve is the memristor with the transition voltage of  $V_{set} = 1.8\text{V}$ . The blue I-V curve is the memristor with the transition voltage of  $V_{set} = 2.2\text{V}$ . (For interpretation of the references to colour in this figure legend, the reader is referred to the web version of this article.)

memristance increases sharply to  $R_{off}$ .

Step 2: the input source  $V_{in}$  is positive, and the current flows through memristor  $R_M$  and reference resistor  $R$  (NMOS can be regarded as open), as shown in Fig. 4. The voltage applied to the memristor is positive (it must match  $|V_{in}| > |V_{set}|$ ), and the voltage value is

$$V_M = \frac{R_M}{R_M + R} * V_{in} \quad (6)$$

when  $V_M > V_{set}$ , memristor SET, the memristance decreases gradually, and the memristor voltage value also decreases gradually, until  $V_M = V_{set}$ . When  $V_M = V_{set}$ , the memristor stops SET, so the memristance does not change and remains a certain value, the memristance value is

$$R_M = \frac{V_{set}}{V_{in} - V_{set}} * R \quad (7)$$

where  $V_{in}$  is the input source,  $V_{set}$  is the memristor SET transition voltage,  $R$  is the reference resistor.

When  $V_{in} = 2V_{set0}, R = R_0, V_{set} = V_{set0}$ , the memristance value can be set to  $R_0$  after the programmable process. Hence, if we want to program the memristor to  $R_0$ , we only need to set the reference resistor  $R = R_0$ .

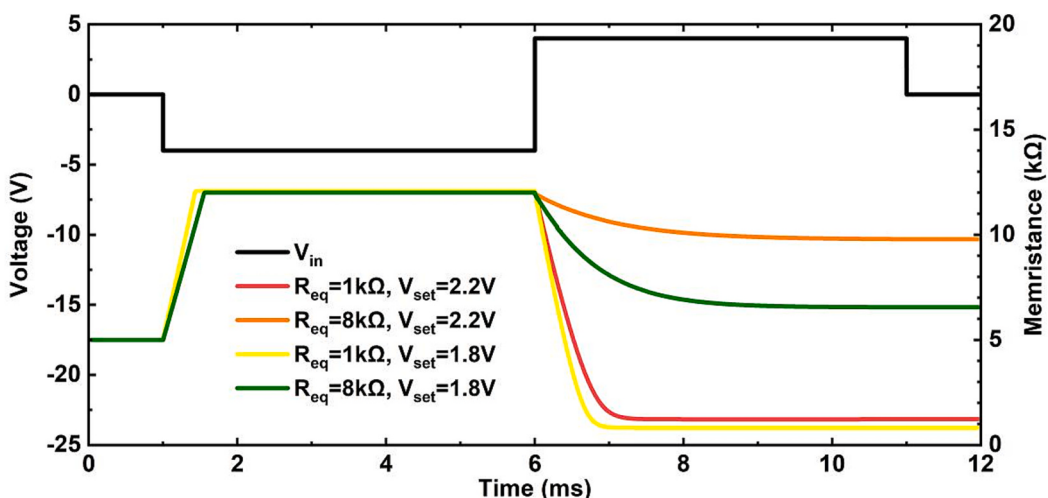


**Fig. 10.** Simulation precision of the circuit. The black line is the input source  $V_{in}$ , and the colour lines are the memristances based on different transition voltage tolerances as the function of stimulation time.

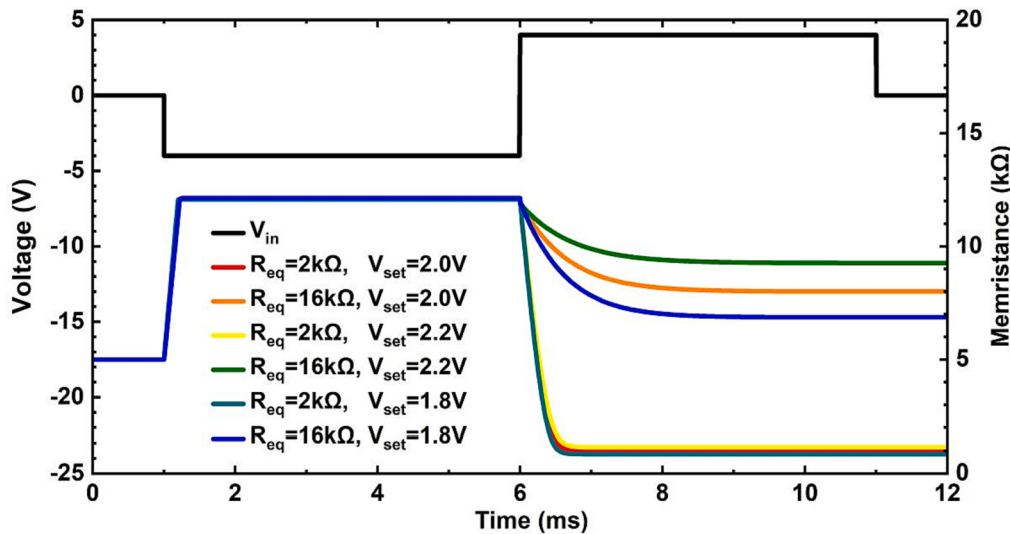


**Fig. 11.** Simulation of the optimized circuit. The black line is the input source  $V_{in}$ , and the colour lines are the memristances evolution based on optimized circuit.

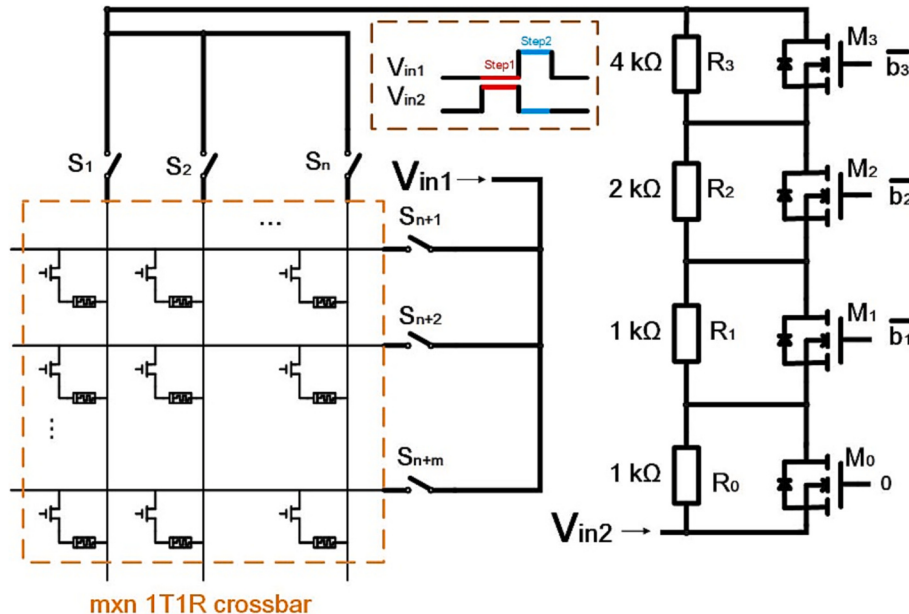


**Fig. 12.** Memristor crossbar programmable circuit.  $S_1, S_2, \dots, S_n$  are the selectors of 1T1R crossbar rows.  $S_{n+1}, S_{n+2}, \dots, S_{n+m}$  are the selectors of 1T1R crossbar columns.  $V_{in1}$  and  $V_{in2}$  are two input sources.

### 2.3. The simulation of the memristor programmable circuit

Fig. 5 shows the simulation result of the memristor programmable circuit. The width of the programming process is 10 ms (To illustrate the circuit, the whole programming time is set to 10 ms as an example. It must reserve enough time for transition, the programming time is must longer than the transition time. For the memristor that has shorter transition time, it can also reduce the programming time accordingly). The first 0-5 ms is the period of Step 1, during which the memristor RESET and the memristance increases to  $R_{off}$ . And the following 5-10 ms is the period of Step 2, during which the memristor SET and the memristance decrease to the aim value. When the reference resistor is  $R = 1\text{k}\Omega$ , the memristance simulation result is  $0.9999\text{k}\Omega$ , compared with reference resistor  $R$ , the accuracy of the simulation result is >99%. When the reference resistor is  $R = 8\text{k}\Omega$ , the memristance simulation result is  $8.0097\text{k}\Omega$ ; corresponding to a >99% simulation accuracy. The

simulation result shows that the programmable circuit function is correct, and the circuit has high precision.

### 3. Reference resistor control circuit

#### 3.1. The reference resistor circuit

As shown in Fig. 6(a), reference resistor structure consists of separate channels. When programming the memristor, only one channel work (controlled by  $b_1-b_8$ ). As shown in Fig. 6(b), reference resistor structure are series of parallel reference-resistor-and-NMOS (controlled by  $\overline{b}_3 \overline{b}_2 \overline{b}_1$ ). When programming the memristor, the equivalent value of reference resistor is obtained from the combination of resistors. Obviously, both structures can achieve the same number of states, but the second structure is better in terms of hardware consumption. Additionally, fewer control signals of the second structure are required. This

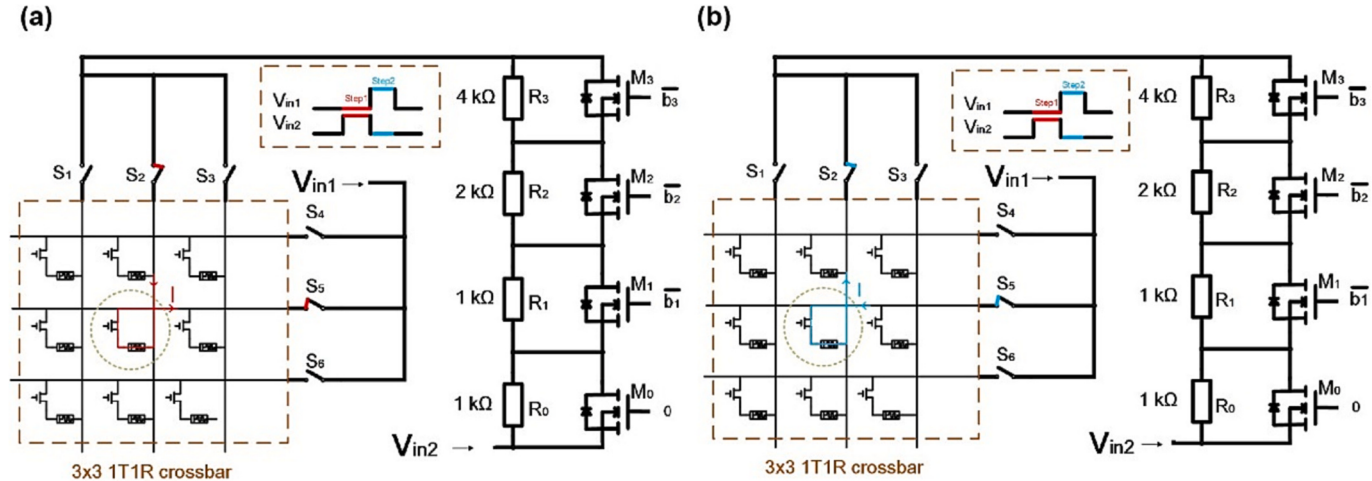


**Fig. 13.** memristor crossbar programmable circuit. The states of selectors  $S_2$  and  $S_4$  are ON; while the states of other selectors are OFF. (a) Step1. In this period, input source  $V_{in1}$  is 0 V and  $V_{in2}$  is 4 V. (b) Step2. In this period, input source  $V_{in2}$  is 0 V and  $V_{in1}$  is 4 V.

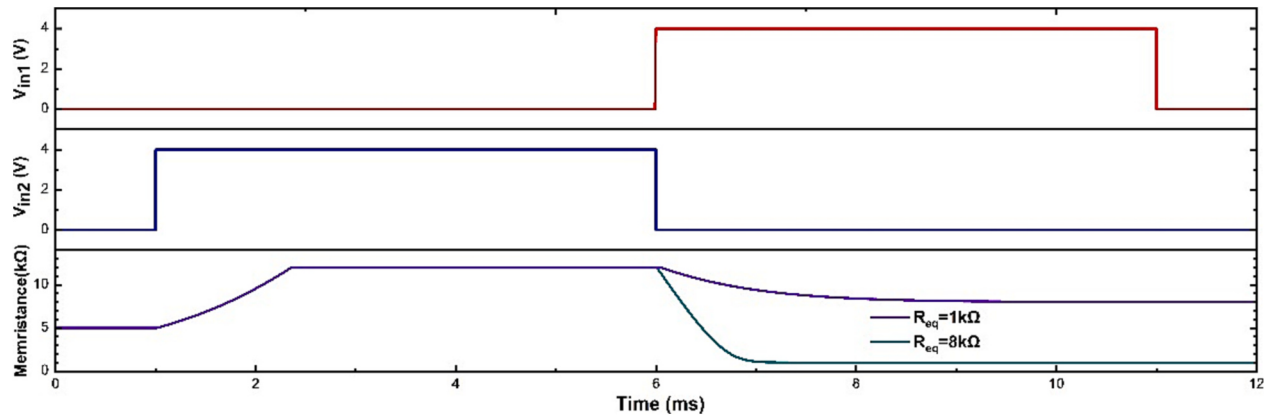


**Fig. 14.** Memristor crossbar programmable circuit simulation. The red line is the source  $V_{in1}$ , and the value is 0 V during 1-6 ms and 4.0 V during 6-11 ms. The blue line is the source  $V_{in2}$ , and the value is 4 V during 1-6 ms and 0 V during 6-11 ms. The purple line represents the memristance evolution when the reference resistor is  $R_{eq} = 8k\Omega$  and the cyan line represents the memristance evolution when the reference resistor is  $R_{eq} = 1k\Omega$ . (For interpretation of the references to colour in this figure legend, the reader is referred to the web version of this article.)

design can improve the flexibility of the reference resistor. After the reference circuit design is completed, there is a fixed correspondence between the digital input signals and the equivalent reference resistance value.

To illustrate the function of the circuit, here are examples of the reference resistance values, and the resistors are selected with  $1k\Omega$ ,  $1k\Omega$ ,  $2k\Omega$ ,  $4k\Omega$ , which may be adjusted according to the actual situation. The four different resistors can achieve different  $R_{eq}$  values. The control signals are  $\overline{b3}\ \overline{b2}\ \overline{b1}$ , which are input digital signals. The reference resistor value is

$$R_{eq} = R_0 + R_1 * \overline{b1} + R_2 * \overline{b2} + R_3 * \overline{b3} \quad (8)$$

where  $R_0, R_1, R_2, R_3$  are reference resistors ;  $\overline{b3}\ \overline{b2}\ \overline{b1}$  are input digital control signals .

The memristor programming circuit can be adjusted to be controlled by more digital input signals, thus the memristor could be programmed to multi-level states. As is shown in Fig. 7,  $\overline{bn} \dots \overline{b1}$  are the control digital signals which can program memristor to multi-level memristance. The reference resistor value is

$$R_{eq} = R_0 + R_1 * \overline{b1} + \dots + R_n * \overline{bn} \quad (9)$$

**Table 1**

The simulation results based on different  $\overline{b3}\ \overline{b2}\ \overline{b1}$  and  $R_{eq}$ .

$\overline{b3}\ \overline{b2}\ \overline{b1}$	$R_{eq}$	Memristance
000	$1 k\Omega$	$1.0001 k\Omega$
001	$2 k\Omega$	$2.0003 k\Omega$
010	$3 k\Omega$	$3.0001 k\Omega$
011	$4 k\Omega$	$4.0016 k\Omega$
100	$5 k\Omega$	$5.0005 k\Omega$
101	$6 k\Omega$	$6.0023 k\Omega$
110	$7 k\Omega$	$7.0045 k\Omega$
111	$8 k\Omega$	$8.0087 k\Omega$

where  $R_0, R_1, \dots, R_n$  are reference resistors ;  $\overline{b1} \dots \overline{bn}$  are digital control signals ;

### 3.2. The simulation of the reference resistor circuit

The simulation results are shown in Fig. 8. The programming time cycle is 10 ms. The first 5 ms is the period of Step 1, and in this period the memristor can be reset to  $R_{off}$ . And the second 5 ms is the period of Step 2, and in this period the memristor will be set to the aim value. When  $\overline{b3}\ \overline{b2}\ \overline{b1} = 000 \sim 111$ , the memristance simulation results are

**Table 2**

Comparison of the programming circuits.

	Performance (Precision)	Power Consumption	Area
Structure in Fig. 6(a)	>99%	$\frac{V_{in}^2}{R_M + R_x}$	$S_{Mem} + 8S_R + 9S_{MOS}$
Structure in Fig. 6(b)	>99%	$\frac{V_{in}^2}{R_M + R_{eq}}$	$S_{Mem} + 4S_R + 4S_{MOS}$

1.0001kΩ, 2.0003kΩ, 3.0001kΩ, 4.0016kΩ, 5.0005kΩ, 6.0023kΩ, 7.0045kΩ, 8.0087kΩ, respectively. All of these simulation results keep 99% programming precision with  $R_{eq}$ .

Table 1 shows the relationship between  $\overline{b3}\ \overline{b2}\ \overline{b1}$  and  $R_{eq}$ ; The digital input signals are  $\overline{b3}\ \overline{b2}\ \overline{b1} = 000 \sim 111$ , and the equivalent reference resistor is  $R_{eq} = 1k\Omega \sim 8k\Omega$ , respectively. The memristance simulation results are also shown in Table 1 and Fig. 8.

### 3.3. The performance, power consumption, and area of the programming circuit

In this section, the programming circuit is analyzed using a 3-bit reference resistor as an example. As in Table 2, it presents the performance, power consumption, and area of the programming circuits. For the precision, it is over 99% (the results of considering the tolerance of other parameters can be found in the analysis in Section 4). Power consumption is determined by input voltage and resistance.  $V_{in}$  is the input voltage,  $R_x$  is the resistor in the channel that is work in the structure in Fig. 6(a), and  $R_{eq}$  is the equivalent resistance in the structure in Fig. 6(b). The area is determined by memristor, resistor, and NMOS.  $S_{Mem}$  is the area of memristor,  $S_R$  is the area of single reference resistor, and  $S_{MOS}$  is the area of single NMOS.

## 4. Precision analysis and simulation

From the formula (7), we know that the tolerances of  $V_{in}$ ,  $V_{set}$ ,  $R$  have an influence on memristance precision. In this paper, we only discuss the tolerance of  $V_{set}$  which is a parameter of memristor intrinsic characteristics. Actually, the parameters that are related to  $V_{set}$  can affect the result. To simplify the analysis, we normalized these parameters to  $V_{set}$ . Considering memristor  $V_{set}$  has 10% tolerance and assuming the ideal value of  $V_{set}$  is  $V_{set0}$ , we discuss two conditions:

Condition 1: memristor  $V_{set}$  has +10% tolerance,

$$V_{set} = V_{set0}(1 + 10\%) = 1.1V_{set0} \quad (10)$$

Condition 2: memristor  $V_{set}$  has -10% tolerance,

$$V_{set} = V_{set0}(1 - 10\%) = 0.9V_{set0} \quad (11)$$

corresponding to blue and red lines in Fig. 9, namely,  $V_{set} = 2.2V$  and  $V_{set} = 1.8V$  based on  $V_{set0} = 2.0V$ .

### 4.1. The impact of $V_{set}$ tolerance

For analysis of the impact of  $V_{set}$ , we also consider memristor  $V_{set}$  has 10% tolerance and assume the ideal value of  $V_{set}$  is  $V_{set0}$ , and  $R_0$  is the aim value. We discuss two conditions:

Condition 1: memristor  $V_{set}$  has +10% tolerance

When  $V_{in} = 2V_{set0}$ ,  $R = R_0$ ,  $V_{set} = V_{set0}(1 + 10\%) = 1.1V_{set0}$ , the memristance value is

$$R_M = 1.222R_0 \quad (12)$$

In Fig. 10, when the positive threshold of the memristor is  $V_{set} = 2.2V$  and the digital input signals are  $\overline{b3}\ \overline{b2}\ \overline{b1} = 000$  ( $R_{eq} = 1k\Omega$ ), the simulation value of memristance is  $R_M = 1.2224k\Omega$ ; when the positive threshold of the memristor is  $V_{set} = 2.2V$  and the digital input signals are

**Table 3**

Memristance precision comparison.

	$V_{set} = V_{set0}$	$V_{set} = 1.1V_{set0}$	$V_{set} = 0.9V_{set0}$
$V_{in} = 2V_{set0}, R = R_0$	0	+22.2%	-18.2%
$V_{in} = 3V_{set0}, R = 2R_0$	0	+15.8%	-14.3%
Precision optimized	0	6.4%	3.9%

$\overline{b3}\ \overline{b2}\ \overline{b1} = 111$  ( $R_{eq} = 8k\Omega$ ), the simulation value of memristance is  $R_M = 9.7921k\Omega$ . The simulation value of memristance conforms to the theoretical value.

Condition 2: memristor  $V_{set0}$  has -10% tolerance

When  $V_{in} = 2V_{set0}$ ,  $R = R_0$ ,  $V_{set} = V_{set0}(1 - 10\%) = 0.9V_{set0}$ , the memristance value is

$$R_M = 0.818R_0 \quad (13)$$

In Fig. 10, when the positive threshold of the memristor is  $V_{set} = 1.8V$  and the digital input signals are  $\overline{b3}\ \overline{b2}\ \overline{b1} = 000$  ( $R_{eq} = 1k\Omega$ ), the simulation value of memristance is  $R_M = 0.8181k\Omega$ ; when the positive threshold of the memristor is  $V_{set} = 1.8V$  and the digital input signals are  $\overline{b3}\ \overline{b2}\ \overline{b1} = 111$  ( $R_{eq} = 8k\Omega$ ), the simulation value of memristance is  $R_M = 6.5496k\Omega$ . The simulation value of memristance also conforms to the theoretical value.

## 5. Optimized circuit

Through the previous analysis, we know the tolerance of  $V_{set}$  has an influence on memristance precision. This proposes a solution to optimize the memristance precision by adjusting the values of  $V_{in}$  and  $R$ . However, it does not need to change the structure of the circuit. For example, when  $V_{in} = 3V_{set0}$ ,  $R = 2R_0$ ,  $V_{set} = V_{set0}$  ( $R_0$  is the aim value,  $V_{set0}$  is the ideal value), it can still precisely program memristance  $R_M = R_0$ . In Fig. 11, when the positive threshold of the memristor is  $V_{set} = 2V$  and the digital input signals are  $\overline{b3}\ \overline{b2}\ \overline{b1} = 000$  ( $R_{eq} = 1k\Omega$ ), the simulation value of memristance is  $R_M = 1.0001k\Omega$ ; when the positive threshold of the memristor is  $V_{set} = 2V$  and the digital input signals are  $\overline{b3}\ \overline{b2}\ \overline{b1} = 111$  ( $R_{eq} = 8k\Omega$ ), the simulation value of memristance is  $R_M = 8.0010k\Omega$ . The memristance simulation results are equal to  $R_{eq}$  with an acceptable error. It proves that this solution is effective. Now, considering the tolerance of  $V_{set}$ , discuss two conditions:

Condition 1: memristor  $V_{set}$  has +10% tolerance

$$\text{When } V_{in} = 3V_{set0}, R = 2R_0, V_{set} = V_{set0}(1 + 10\%) = 1.1V_{set0}$$

$$R_M = 1.158R_0 \quad (14)$$

In Fig. 11, when the positive threshold of the memristor is  $V_{set} = 2.2V$  and the digital input signals are  $\overline{b3}\ \overline{b2}\ \overline{b1} = 000$  ( $R_{eq} = 1k\Omega$ ), the simulation value of memristance is  $R_M = 1.1576k\Omega$ ; when the digital input signals are  $\overline{b3}\ \overline{b2}\ \overline{b1} = 111$  ( $R_{eq} = 8k\Omega$ ), the simulation value of memristance is  $R_M = 9.2626k\Omega$ ; the simulation value of memristance conforms to the theoretical value.

Condition 2: memristor  $V_{set}$  has -10% tolerance

$$\text{When } V_{in} = 3V_{set0}, R = 2R_0, V_{set} = V_{set0}(1 - 10\%) = 0.9V_{set0}$$

$$R_M = 0.857R_0 \quad (15)$$

In Fig. 11, when the positive threshold of the memristor is  $V_{set} = 1.8V$  and the digital input signals are  $\overline{b3}\ \overline{b2}\ \overline{b1} = 000$  ( $R_{eq} = 1k\Omega$ ), the simulation of memristance is  $R_M = 0.8569k\Omega$ ; when the digital input signals are  $\overline{b3}\ \overline{b2}\ \overline{b1} = 111$  ( $R_{eq} = 8k\Omega$ ), the simulation of memristance is  $R_M = 6.8611k\Omega$ ; the simulation value of memristance also conforms to the theoretical value. Condition 1 and condition 2 confirm that properly adjusting the values of  $V_{in}$  and  $R$  can optimize the memristance precision. However, it needs a higher voltage value of source  $V_{in}$ , so it should make a tradeoff between memristance precision and input voltage value. Memristance precision comparison is in Table 3.

**Table 4**  
Simulation result of memristance.

	$V_{set} = V_{set0}$	$V_{set} = 1.1V_{set0}$	$V_{set} = 0.9V_{set0}$
	$R_0 = 1k\Omega$	$R_0 = 8k\Omega$	$R_0 = 1k\Omega$
$V_{in} = 2V_{set0}, R = R_0$	1.0001kΩ	8.0087kΩ	1.2224kΩ
$V_{in} = 3V_{set0}, R = 2R_0$	1.0001kΩ	8.0010kΩ	1.1576kΩ

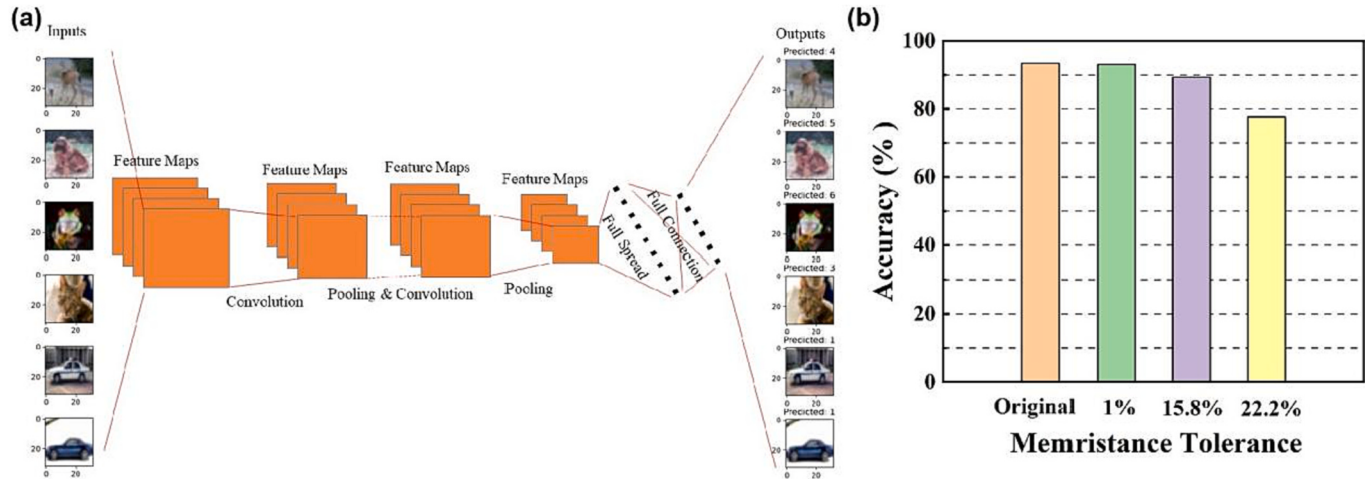


Fig. 15. (a) A CNN architecture for images recognition; (b) Computing accuracy of the different memristance tolerance.

Simulation result of memristance is in Table 4.

## 6. Memristor crossbar programming circuit

Besides the single memristor device, our programming circuit can also be used to control the memristor crossbar precisely. For example, as shown in Fig. 12, in an  $m \times n$  1T1R memristor crossbar, the row signals are controlled by selectors  $S_1, S_2, \dots, S_n$ , and the column signals are controlled by selectors  $S_{n+1}, S_{n+2}, \dots, S_{n+m}$ . Through selecting specific row signal and column signal, it can program specific memristor in the memristor crossbar precisely. For example, to select the memristor that is in the second row and the second column, selectors  $S_2$  and  $S_{n+2}$  are ON, while the other selectors are OFF. It also takes two steps to program the memristor. In addition, in the former structure, it uses a single source ( $V_{in}$ ) to program the memristor where a negative pulse is necessary. Here, we use two sources ( $V_{in1}$  &  $V_{in2}$ ) to stimulate the memristor crossbar and these sources are all positive bias.

There are also two steps to program the memristor which is illustrated as follows. Taking an example on a  $3 \times 3$  1T1R memristor crossbar and the memristor in the second row and second column needs to be updated. In Step1, as in Fig. 13(a),  $V_{in1}$  is 0 V and  $V_{in2}$  is 4 V which triggers memristance increases sharply until to  $R_{off}$ , the memristor completes RESET process. In Step2, as in Fig. 13(b),  $V_{in1}$  is 4 V while the  $V_{in2}$  is 0 V which makes the memristance of the memristor is programmed to aim value gradually, and the memristor completes the programming process. The programming process for the other memristors is similar.

Fig. 14 are simulation waveforms, 1-6 ms is Step 1, and 6-11 ms is Step 2. When the positive threshold of the memristor is  $V_{set} = 2V$  and the digital input signals are  $\overline{b3}\ \overline{b2}\ \overline{b1} = 000$  ( $R_{eq} = 1k\Omega$ ), the simulation value of memristance is  $R_M = 0.9998k\Omega$ ; when the digital input signals are  $\overline{b3}\ \overline{b2}\ \overline{b1} = 111$  ( $R_{eq} = 8k\Omega$ ), the simulation value of memristance is  $R_M = 8.008k\Omega$ . The simulation results agree with the aim values and the precision is  $>99\%$ .

## 7. Application

With the advent of the big data era, the scale of information has been explosive growth. And the scale of image data is also increasing explosively. However, in the conventional computing architecture, computation and storage is physically separate. It requires frequent data shuttling among the computation and storage units, which causing significant system consumption and speed loss. Hence, it is difficult to emulate the requirements of information analysis and processing [25–27]. Memristors with nonvolatility and integrated storage-and-computation properties can be used to build intelligent processing systems that are closer to the structure and function of biological brains [28,29]. They are also of great significance for achieving the integrated storage and computation for image data [30].

As Fig. 15(a), it is a CNN architecture for image recognition based on memristor crossbar arrays. Inputs are images for recognition, and outputs are the results of recognition. On platform MNSIM [31], we analyzed the computing accuracy of different memristance tolerance. The algorithm uses VGG8 and the dataset uses CIFAR10. The size of input image is  $28 \times 28$ , hence, the network consists of 784 input neurons. In addition, the numbers of convolution layers and pooling layers are 8 and 5, respectively. And 10 output neurons are corresponding to 10 kinds of classification targets. Hardware configuration is Intel Xeon Gold 6248 @2.50GHz CPU. System is Windows Server 2019 and its word length is 64 bits.

Taking 10% tolerance of  $V_{set}$  into consideration, as mentioned in Table 2, the memristance tolerances of the circuit before and after optimization are 22.22% and 15.8%. Hence, we analyzed the computing accuracy of three memristance tolerance 1%, 15.8%, and 22.2%. As Fig. 15(b), the computing accuracy is 93.45% (original accuracy). For computing based on memristor crossbar arrays, when the memristance tolerance is 1%, the computing accuracy is 93.09%, and the computing accuracy decreased to 89.36% and 77.64% with the memristance tolerance of 15.8% and 22.22%, respectively. The latency of the network training directly by traditional computer is about 7.47 s, while this value

**Table 5**

Hardware area.

Hardware Area(mm <sup>2</sup> )- Total: 1399.0					
Memristor Crossbar	ADC	DAC	Buffer	Pooling	Other Digital Parts
1353.0	2.15	0.15	33.3	2.6	7.9

**Table 6**

Hardware power consumption.

Hardware Power Consumption(W)- Total: 9.38					
Memristor Crossbar	ADC	DAC	Buffer	Pooling	Other Digital Parts
0.0009	2.8	2.7	3.6	0.01	0.21

decreased to 62.155 ms based on memristor crossbar arrays, and the time efficiency improved >119 times. As in [Table 5](#), it is the hardware area of different parts; as in [Table 6](#), it is the hardware power consumption of different parts. Other digital parts include adder, MUX, register and so on.

## 8. Conclusion

In this paper, a novel memristor programming circuit with a reference resistor structure is proposed which can achieve precise memristance, and the function of the circuit has been fully verified by simulation. Just as the memristance adjustment is sensitive to the memristor  $V_{set}$ , this paper analyzed the precision of the memristance under the memristor  $V_{set}$  has  $\pm 10\%$  tolerance, and proposed a solution to improve the memristance precision at the cost of increasing input voltage value without changing the circuit structure. In order to complete the circuit design, it should make a tradeoff between the memristance precision and the input voltage value. In addition, this paper demonstrates that the circuit can be applied to the memristor crossbar and the simulation results of the circuit verify the programming function on the memristor crossbar. In the end, this paper analyzed the computing accuracy of different memristance tolerance in the CNN image recognition based on memristor crossbar arrays.

## CRediT authorship contribution statement

**Shengtao Tu:** Conceptualization, Methodology, Validation, Formal analysis, Investigation, Data curation, Writing – original draft. **Jinyu Li:** Software. **Yanyun Ren:** Data curation, Writing – review & editing. **Qin Jiang:** Visualization, Writing – review & editing. **Shisheng Xiong:** Resources, Supervision, Project administration, Funding acquisition, Writing – review & editing.

## Declaration of Competing Interest

The authors declare no conflict of interest.

## Data availability

Data will be made available on request.

## Acknowledgements

The work was supported by National Natural Science Foundation of China (Nos. U20A20227).

## References

- [1] L. Chua, Memristor-the missing circuit element, *IEEE Trans. Circ. Theory* 18 (5) (1971) 507–519.
- [2] D.B. Strukov, G.S. Snider, D.R. Stewart, R.S. Williams, The missing Memristor found, *Nature* 453 (7191) (2008) 80–83.
- [3] Q. Jiang, Y. Ren, Z. Cui, Z. Li, L. Hu, R. Guo, S. Duan, F. Xie, G. Zhou, S. Xiong, Csppbr3 perovskite quantum dots embedded in polystyrene-Poly2-vinyl pyridine copolymer for robust and light-tunable Memristors, *ACS Appl. Nano Mater.* 6 (10) (2023) 8655–8667.
- [4] X. Yang, B. Taylor, A. Wu, Y. Chen, L.O. Chua, Research progress on memristor: from synapses to computing systems, in: *IEEE Transactions on Circuits and Systems I: Regular Papers* 69(5), 2022, pp. 1845–1857.
- [5] X. Ji, Z. Dong, C.S. Lai, D. Qi, A brain-inspired in-memory computing system for neuronal communication via memristive circuits, *IEEE Commun. Mag.* 60 (1) (2022) 100–106.
- [6] Y. Zhong, J. Tang, X. Li, X. Liang, Z. Liu, Y. Li, Y. Xi, P. Yao, Z. Hao, B. Gao, et al., A Memristor-based analogue reservoir computing system for real-time and power-efficient signal processing, *Nat. Electron.* 5 (10) (2022) 672–681.
- [7] S. Zhang, Y. Zhao, Q. Chen, Y. Wang, J. Jiang, Y. Wang, Y. Fu, Q. Liu, Q. Wang, D. He, A perovskite-based artificial photonic synapse with visible light modulation and ultralow current for neuromorphic computing, *Microelectron. Eng.* 274 (2023), 111982.
- [8] Z. Dong, X. Ji, G. Zhou, M. Gao, D. Qi, Multimodal neuromorphic sensory-processing system with memristor circuits for smart home applications, *IEEE Trans. Ind. Appl.* 59 (1) (2023) 47–58.
- [9] A.V. Emelyanov, K.E. Nikiruy, V.A. Demin, V.V. Rylkov, A.I. Belov, D.S. Korolev, E.G. Gryaznov, D.A. Pavlov, O.N. Gorshkov, A.N. Mikhaylov, et al., Yttria-stabilized zirconia cross-point memristive devices for neuromorphic applications, *Microelectron. Eng.* 215 (2019), 110988.
- [10] W. Wang, G. Zhou, Moisture influence in emerging neuromorphic device, *Front. Phys.* 18 (5) (2023) 53601.
- [11] G. Zhou, X. Ji, J. Li, F. Zhou, Z. Dong, B. Yan, B. Sun, W. Wang, X. Hu, Q. Song, et al., Second-order associative memory circuit hardware implemented by the evolution from battery-like capacitance to resistive switching memory, *iScience* 25 (10) (2022), 105240.
- [12] Y.V. Pershin, M.D. Ventra, Practical approach to programmable analog circuits with memristors, in: *IEEE Transactions on Circuits and Systems I: Regular Papers* 57(8), 2010, pp. 1857–1864.
- [13] R. Berdan, T. Prodromakis, C. Toumazou, High precision analogue Memristor state tuning, *Electron. Lett.* 48 (18) (2012) 1105–1107.
- [14] E.J. Merced-Grafals, N. Dávila, N. Ge, R.S. Williams, J.P. Strachan, Repeatable, accurate, and high speed multi-level programming of Memristor 1t1r arrays for power efficient analog computing applications, *Nanotechnology* 27 (36) (2016), 365202.
- [15] K.M. Kim, J.J. Yang, J.P. Strachan, E.M. Grafals, N. Ge, N.D. Melendez, Z. Li, R.S. Williams, Voltage divider effect for the improvement of variability and endurance Oftaox Memristor, *Sci. Rep.* 6 (1) (2016) 20085.
- [16] I. Vourkas, J. Gómez, Á. Vasilieadis, G.C. Sirakoulis, A. Rubio, Exploring the voltage divider approach for accurate memristor state tuning, in: 2017 IEEE 8th Latin American Symposium on Circuits & Systems (LASCAS), 2017, pp. 1–4.
- [17] I. Vourkas, J. Gomez, A. Abusleme, G.C. Sirakoulis, A. Rubio, Voltage divider for self-limited analog state programing of memristors, in: 2020 IEEE International Symposium on Circuits and Systems (ISCAS), 2020, 1–1.
- [18] O.A. Olumodeji, M. Gottardi, A pulse-based memristor programming circuit, in: 2017 IEEE International Symposium on Circuits and Systems (ISCAS), 2017, pp. 1–4.
- [19] S.M.A. Mokhtar, W.F.H. Abdullah, K.A. Kadiran, R. Rifin, M. Omar, Write and read circuit for memristor analog resistance switching, in: 2017 IEEE 8th Control and System Graduate Research Colloquium (ICSGRC), 2017, pp. 13–16.
- [20] M. Tarkhan, M. Maymandi-Nejad, S.H. Klidbary, S.B. Shouraki, A bridge technique for memristor state programming, *Int. J. Electron.: Theor. Exp.* 107 (4/6) (2020) 1015–1030.
- [21] A.A. Daoud, A.S. Dessouki, H. Mostafa, R.M. Abdallah, E.-S.M. El-Rabaie, A high precision write/read circuits for memristors using digital input/output interfaces, *Microelectron. J.* 96 (2020), 104694.
- [22] A. Cirera, C. Fernandez, I. Vourkas, A. Rubio, Exploring different circuit-level approaches to the forming of resistive random access memories, in: 2022 11th International Conference on Modern Circuits and Systems Technologies (MOCAST), 2022, pp. 1–4.
- [23] J.L. Randrianantaina, A.Y. Baran, N. Korkmaz, R. Kiliç, Functional emulator designs for a memristor model with programmable analog and digital platforms, *J. Comput. Electron.* 22 (1) (2023) 519–530.
- [24] Y.V. Pershin, M. Di Ventra, Spice model of memristive devices with threshold, *Radioengineering* 22 (2) (2013) 485–489.
- [25] M.A. Zidan, J.P. Strachan, W.D. Lu, The future of electronics based on Memristive systems, *Nat. Electron.* 1 (1) (2018) 22–29.
- [26] Z. Wang, S. Joshi, S.E. Savel'ev, H. Jiang, R. Midya, P. Lin, M. Hu, N. Ge, J. P. Strachan, Z. Li, et al., Memristors with diffusive dynamics as synaptic emulators for neuromorphic computing, *Nat. Mater.* 16 (1) (2017) 101–108.
- [27] Z. Dong, C.S. Lai, Z. Zhang, D. Qi, M. Gao, S. Duan, Neuromorphic extreme learning machines with bimodal memristive synapses, *Neurocomputing* 453 (2021) 38–49.
- [28] C.D. Schuman, T.E. Potok, R.M. Patton, J.D. Birdwell, M.E. Dean, G.S. Rose, J. S. Plank, A survey of neuromorphic computing and neural networks in hardware, *ArXiv* (2017) abs/1705.06963.

- [29] M. Davies, N. Srinivasa, T.H. Lin, G. Chinya, Y. Cao, S.H. Choday, G. Dimou, P. Joshi, N. Imam, S. Jain, et al., Loihi: a neuromorphic manycore processor with on-chip learning, *IEEE Micro* 38 (1) (2018) 82–99.
- [30] R. Su, R. Xiao, C. Shen, D. Song, J. Chen, B. Zhou, W. Cheng, Y. Li, X. Wang, X. Miao, Oxygen ion migration induced polarity switchable Srfeox memristor for high-precision handwriting recognition, *Appl. Surf. Sci.* 617 (2023), 156620.
- [31] L. Xia, B. Li, T. Tang, P. Gu, P.Y. Chen, S. Yu, Y. Cao, Y. Wang, Y. Xie, H. Yang, MnSim: simulation platform for memristor-based neuromorphic computing system, in: *IEEE Transactions on Computer-Aided Design of Integrated Circuits and System* 37(5), 2018, pp. 1009–1022.